








Research Article

Dynamic Variation in Hippocampal Metabolism after Acute Stress Exposure: An In Vivo Proton Magnetic Resonance Spectroscopy Study at 9.4 T

Yoon Ho Hwang ¹, Min-Hee Lee ², Chang-Soo Yun ³, Yong-Tae Kim ⁴,
Hyeon-Man Baek ⁴, Bong Soo Han ³ and Dong Young Kim ¹

¹Department of Biomedical Engineering, Yonsei University, Wonju 26493, Republic of Korea

²Institute of Human Genomic Study, Korea University Ansan Hospital, Ansan 15355, Republic of Korea

³Department of Radiation Convergence Engineering, Yonsei University, Wonju 26493, Republic of Korea

⁴Department of Basic Medical Sciences, Lee Gil Ya Cancer and Diabetes Institute, Gachon University, Incheon 21999, Republic of Korea

Correspondence should be addressed to Dong Young Kim; dongkim77@yonsei.ac.kr

Received 5 July 2021; Revised 10 September 2021; Accepted 25 September 2021; Published 20 October 2021

Academic Editor: Nives Galić

Copyright © 2021 Yoon Ho Hwang et al. This is an open access article distributed under the Creative Commons Attribution License, which permits unrestricted use, distribution, and reproduction in any medium, provided the original work is properly cited.

An acute stress response is a complex process that activates the neuroendocrine and metabolic systems for homeostasis. A study on acute stress is important to understand how an organism adapts to stress for survival. However, most studies have focused on chronic stress, and there are few studies on acute stress. They have analyzed the metabolic alterations in the brain at a particular time after acute stress. This study explored the temporal variations of the brain metabolites in the hippocampus after acute restraint stress using proton magnetic resonance spectroscopy. All mice in the acute stress group were physically restrained for two hours in a 50 mL conical tube. A 9.4 T animal MRI and MRS scanner was used with point-resolved spectroscopy technique for data acquisition, which was repeated four times without interscan interval. Metabolites were quantified from the data using LCMoDel with a simulated basis set. Based on the change in concentration of metabolites, the data were statistically analyzed using two-way repeated-measures analysis of variance between groups and a support vector machine for all time points and Student's *t*-test with FDR correction for each time point. The present study found that the differences between groups are significantly ($P < 0.05$) presented in alanine and glutamate. The effect of time of the two metabolites significantly exists ($P < 0.05$): the first, second, and third time points in alanine and the first and second time points in glutamate. A combination of stress-specific metabolites (alanine, glutamate, N-acetyl-aspartate) that best reflect the influence of acute stress was determined using a support vector machine. These findings may indicate the importance of the timing of analysis after acute stress and provide new insights into a deeper understanding of acute stress response, including the molecular mechanism of stress-related disorders and stress resilience or vulnerability.

1. Introduction

The stress response is defined as a neurochemical process, which is an adaptive or maladaptive reaction to alterations in the external environment (e.g., stressful situations or events) that threaten the physiological homeostasis of the brain for the survival of living organisms [1–5]. External stimuli triggering the stress response are characterized as different

types of stressors (physical, pharmacological, psychological, and social) [6, 7]. Depending on the stress-induced time by one or more stressors, stress is classified as acute or chronic. As most of the previous studies have focused on chronic stress [8, 9], the importance of the effects of acute stress has not emerged and there are only a few related studies [10–13].

Acute stress is based on a single stressor that generates an intense stimulus once producing negative structural and

functional changes in the brain [14–18]. The influence of acute stress in the brain may result in morphological changes such as hippocampal volume loss [19], apical dendritic retraction [20], reduced activity of antioxidant enzymes [12], neurotoxicity due to the overactivation of glutamate release [21–24], and diminished cell proliferation [7, 25]. The effects of acute stress in the brain are caused by atypical physiological responses leading to stress-related disorders. These results raise the necessity of investigation into the maladaptive pathways involved in the acute stress response [5, 26, 27]. In addition, as the acute stress response is the underlying response to chronic stress as well as nature's fundamental mechanism for survival, the study of acute stress is essential to develop a deep understanding of the harmful effects caused by chronic stress and the basal mechanism of stress-related disorders [28].

In regard to stress, the hippocampus is considered an important region in the brain regulating the activation of the hypothalamic-pituitary-adrenal axis based on stress hormones such as glucocorticoids (e.g., corticosterone or cortisol) along with the medial prefrontal cortex [4]. The region is particularly vulnerable and susceptible to acute stress, which may lead to neurogenesis inhibition, neurochemistry alterations, neuron excitability changes, and/or neuron death [16]. Previous studies reported that acute stress in a rat brain induced changes in the concentration of metabolites [29, 30]. Gandhi et al. found that there are significant metabolic alterations in the urine due to acute cold stress with a 9.4 T NMR spectrometer [29]. Shi et al. found that trimellitic anhydride decreased in the FST-1d model compared with the control based on a 14.1 T NMR spectrometer [30]. The *ex vivo* experiments using high-field NMR may provide more accurate and reliable information on the concentrations of metabolites in the rat brain than *in vivo* experiments. However, *ex vivo* experiments are inappropriate to apply studies that analyze the effects of acute stress on living organisms because they sacrifice animals to prepare dissected brain samples of the regions of interest. Therefore, noninvasive *in vivo* experiments using proton magnetic resonance spectroscopy (^1H -MRS) are needed. Recent *in vivo* studies have investigated the metabolic changes in the rodent brain after exposure to acute stress using ^1H -MRS [11, 31]. Kim et al. found significantly increased glutamate levels in the cerebral cortex and hippocampus of the rat brain following acute restraint stress, and glutamate levels returned to the normal state in the hippocampus but not in the cerebral cortex after a 1-h recovery period from 1-h restraint stress [11]. Gapp et al. reported that a mouse exposed to acute cold swim stress during early life stages showed reduced concentrations of N-acetyl-aspartate, glutamate, and γ -aminobutyrate in the prefrontal cortex using 14.1 T ^1H -MRS [31].

While these ^1H -MRS studies provided evidence on metabolic alterations induced by acute stress in the brain using endpoint analysis [6], these cross-sectional studies could not investigate metabolic dynamics for the response to acute stress over time. Houtepen et al. [13] reported that (1) mean glutamate and γ -aminobutyric acid levels varied over time in the control group, (2) the difference between both

groups after acute stress and the difference in glutamate levels before and after acute stress in the stress group were not similar [13]. These results support that comparing both groups only at any specific time point can lead to bias and by chance in the analyzed results. Therefore, metabolic dynamics over time are important for acute stress [32]. Physiological variations induced by acute stress in the brain occur over time, including hormonal changes, classified as short-term and long-term effects of acute stress. These prolonged changes may be relevant for stress-related disorders with structural (e.g., dendritic retraction) and functional (e.g., glutamate release) consequences. This finding raises the necessity for investigating the metabolic changes of the acute stress response over time [5].

Recently, machine learning (ML) techniques have been introduced that have been used in various fields to select the metabolites that better characterize the effects of acute stress. One of the methods of ML, a support vector machine (SVM), is a supervised learning technique that divides into two different classes using a hyperplane (or decision boundary) that maximizes the margin between data in a two-dimensional or more feature space [33]. It is a powerful tool for subtle pattern recognition and classification [34]. Moreover, the SVM has the advantage of being less error data impact and less overfitting by adjusting the cost (C) parameter. This elicits that using the SVM, metabolites that best describe the effects of acute stress by better classifying both groups can be selected from time-series *in vivo* data.

Our primary hypothesis is that acute stress impacts the metabolic dynamics of the brain; then stress-specific changes in the concentration of metabolites occur over time. Based on ^1H -MRS data acquired over time, the present study investigates (1) which metabolites differ in metabolic dynamics between control and acute stress groups, (2) the period that accurately reflects a variation in the characteristics of the metabolites in the hippocampus after acute stress exposure, and (3) the metabolites that are most influenced by acute stress through feature selection using the SVM. To our knowledge, this is the first study to investigate a dynamic variation in the metabolites after inflicting restraint stress in the mouse brain. Furthermore, our proposed noninvasive approach could help explore the effects of acute stress on metabolites in human research.

2. Materials and Methods

2.1. Experimental Animals. Male C57BL/6N mice (ORIENT BIO Inc., South Korea) with body weight over 18 g and below 25 g at 4 weeks of age were used as experimental animals. The mice were housed three per transparent plastic cage and allowed to acclimatize for 2 weeks before the ^1H -MRS experiment to adapt to the environment and minimize the stress resulting from an unfamiliar situation. The mice had unconstrained access to water and food and were maintained under controlled temperature (21–23°C) and humidity (50–60%) with a 12-h light/12-h dark cycle (light on from 06:00 to 18:00). The mice were randomly divided into a control group ($N = 12$) and a stress group ($N = 12$). All experiments were approved by the Institutional Animal Care

and Use Committee and conducted at the Lee Gil Ya Cancer and Diabetes Institute accredited by the Association for Assessment and Accreditation of Laboratory Animal Care International that uses international standards for animal care and use globally. All procedures for experiments were in compliance with the Center of Animal Care and Use in Animal research (guidelines for animal users).

2.2. Restraint Stress Protocol. As shown in Figure 1(a), based on the stress protocol reported by previous studies [35, 36], 12 mice were exposed to acute restraint stress physically for 2 hours in a transparent 50 mL conical plastic centrifuge tube (3 cm in diameter and 10 cm in length) with openings toward the body (3 mm in diameter) and mouth (5 mm in diameter) of the mice to create airflow for ventilation with background noise in an air-conditioned room for the period of restraint. The residual space in the tube was filled to create pressure and minimize mouse movement for perfect immobility. The body and head were fixed to make the mice immovable and create an inescapable space. After completing the restraint procedure, the mice were used for *in vivo* ^1H -MRS data acquisition. The mice in the control group were not exposed to restraint stress and maintained in the cage until the initiation of the ^1H -MRS experiment.

2.3. Proton Magnetic Resonance Spectroscopy. ^1H -MRS experiment was performed using ParaVision 5.0 software under Red Hat Linux based on Bruker BioSpec Avance III 94/20 USR (Bruker BioSpin MRI GmbH, Ettlingen, Germany) with a 9.4 T horizontal 200 mm bore magnet (inner diameter: 114 mm) and 660 mT/m actively shielded gradient coil at cell to *in vivo* imaging core-facility research center as shown in Figure 1(b). Excitation resonating at 400 MHz was conducted using a volume transmit-only resonator. A receive-only surface coil (2 × 2 array coil) was used for the reception of signals from the mouse brain.

Each experiment in both groups was conducted alternatively, three mice at a day. Excluding other processes such as brain positioning in the center of the magnet, shimming, voxel positioning, and acquisition of unsuppressed water signal, ^1H -MRS data were acquired every 34 minutes at 4 consecutive time points in both groups. Spontaneously respiring mice were anesthetized with 4.0% isoflurane at the introduction and 1.0–2.0% isoflurane during the experiment in a 1 : 2 O_2 : air mixture. The mice were placed on a flat MR bed in a prone position. The mouse brain was tightly fixed with a glass bite bar and 2 plastic ear inserts. A water-heated body-warming system was applied to the mouse to prevent the risk of hypothermia during anesthesia [37]. The whole body of the mouse was maintained at a constant temperature via a cover connected to the water-circulating equipment that set the distilled water to 38°C [38]. The rate of respiration was monitored in real time with MR-compatible instruments (SA Instruments, Inc., Stony Brook, NY, USA) to adjust anesthetic concentrations and maintain a stable condition.

To localize the desired voxel of interest (VOI), T2-weighted images were acquired using rapid acquisition with relaxation enhancement (RARE) with the following

acquisition parameters: TR = 5000 ms, $\text{TE}_{\text{eff}} = 48$ ms, RARE factor = 8, NA = 1, FOV = $3 \times 3 \text{ cm}^2$, slice thickness = 1 mm, matrix size = 256×256 , 36 slices (axial = 12, sagittal = 12, coronal = 12). The VOI ($1.8 \times 3.4 \times 1.8 \text{ mm}^3$, $11.016 \mu\text{L}$) was placed to include most of the hippocampus, an area related to stress through the anatomical images as shown in Figure 1(b). For uniform homogeneity of the magnetic field inside the VOI, the shim (first and second order) was adjusted automatically using a fast and automatic shimming technique by mapping along with projections. The procedure for automated shim was repeated until the linewidth of the resulting water signal was below 14 Hz. A point-resolved spectroscopy (PRESS) was used for the acquisition of ^1H -MRS data from a single voxel with the following acquisition parameters: TR = 4000 ms, TE = 10 ms, NA = 512, complex points = 4096, spectral width = 5000 Hz, including that the bandwidth of the excitation/refocusing RF pulse is 5600 Hz to minimize the chemical shift displacement error in the higher magnetic field. The predominant water signal inside the VOI was suppressed by variable power RF pulses with optimized relation delays to detect metabolite signals [11, 39]. An outer volume suppression scheme was performed for the minimization of artifacts caused by the unwanted signals outside the VOI. The eight averaged unsuppressed water signals were acquired in the same manner and VOI as ^1H -MRS data [40]. Additionally, the compensation of eddy current [41] due to strong gradient fields and phase correction was applied during data acquisition [42] for distortion resulting from combining the RF signals with a different phase in the surface coil. When 512 scans were obtained and one averaged raw datum was computed with one, a procedure for frequency drift like the alignment of each scan was performed due to the long acquisition time.

2.4. Metabolite Quantification. As shown in Figure 1(c), the ^1H -MRS data corrected were analyzed with the linear combination analysis method (LCModel) [43, 44] to calculate the concentration of brain metabolites by fitting the experimentally obtained ^1H -MRS data based on eight averaged unsuppressed water signal and a simulated basis set provided by the LCModel. The simulated macromolecule signal and the following metabolites were included in the simulated basis set: alanine (Ala), aspartate (Asp), creatine (Cr), γ -aminobutyric acid (GABA), glucose (Glc), glutamine (Gln), glutamate (Glu), glycerophosphorylcholine (GPC), glutathione (GSH), *myo*-inositol (*m*-Ins), lactate (Lac), phosphorylcholine (PCh), phosphocreatine (PCr), *scyllo*-inositol (*s*-Ins), N-acetylaspartate (NAA), N-acetylaspartylglutamate (NAAG), and taurine (Tau). Among the basis spectra in the simulated basis set, *s*-Ins was excluded from the process of quantification using the LCModel because it had a smaller concentration (<1 mM) in the mouse brain and nothing to do with the acute stress [45]. Also, ascorbate (Asc), phosphorylethanolamine (PE), and glycine (Gly) were excluded from the analysis based on the LCModel because these metabolites were not related to acute stress and it was difficult to detect for the following reasons: (1)

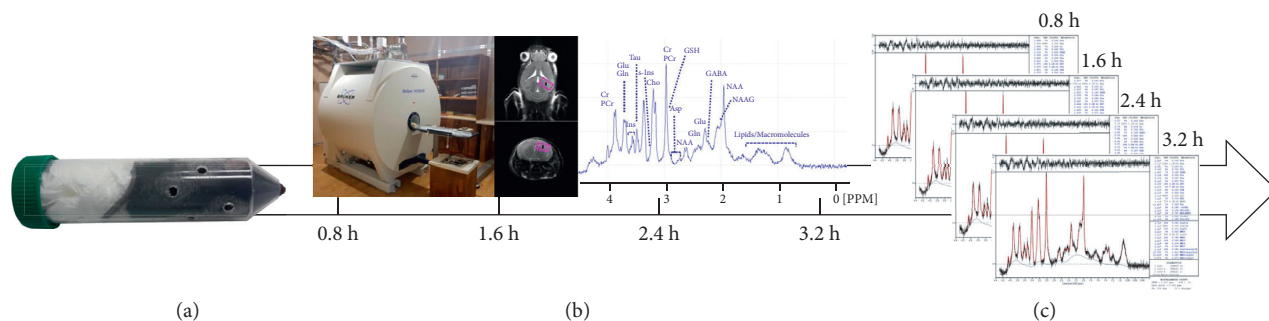


FIGURE 1: A flowchart of ^1H -MRS data analysis: from data acquisition to metabolite quantification. (a) Mouse in the stress group was exposed to acute restraint stress physically for 2 hours in a transparent 50 mL conical tube. (b) ^1H -MRS data in the hippocampus were collected at 4 consecutive time points using 9.4 T Bruker MRI. (c) Metabolites were quantified using the linear combination analysis method (LCModel) in four time points.

smaller concentration (Asc: about 1 mM [46]; PE: 1~2 mM; Gly: <1 mM [46, 47]), (2) overlap with other metabolites (Asc: Glu, Gln, and GSH [48]; PE: other phospholipids with similar structures; Gly: *m*-Ins [47]), and (3) multiplicity (Asc: multiplet at 3.73 and 4.01 ppm [48]; PE: multiplet at 3.22 and 3.98 ppm [47]). Using the LCModel, the concentrations of metabolites were calculated from the ^1H -MRS data using a prior knowledge about the chemical shift of each metabolite (e.g., simulated basis set) and the unsuppressed water signal for water scaling. When the metabolites were quantified by the LCModel, the unsuppressed water signal was used as an internal reference and its attenuation by relaxation and other effects was applied by multiplying the gain correction factor (ATTH2O: 0.01094). The ^1H -MRS data were analyzed at a range between 0.2 ppm and 4.3 ppm for the most discriminating metabolites. Spectral fitting was evaluated by the signal-to-noise ratio (SNR) and Cramer–Rao lower bound (CRLB). CRLB was the estimated standard error in percent of the estimated concentration of metabolites through the spectral registration by the LCModel. If the SNR was below 10 [11], and the CRLB for metabolites and time points was over 20% as recommended by the LCModel [49], the ^1H -MRS data were excluded from the statistical analysis to minimize bias in the results of inaccurate quantification.

2.5. Feature Selection. SVM, one of the machine learning algorithms, is a powerful classifier that separates two distinguishable classes based on the support vectors and the optimal hyperplane divided with the maximum margin [50]. The SVM with a linear kernel was used to select the features that best explain the effect of acute stress by dividing the control group and stress group. Each of the metabolites quantified through the LCModel was considered one feature with each dimension and independent variable; the area under the concentration curve (AUC) of consecutive four time points for each metabolite was calculated with numerical integration via the trapezoidal method. The optimal number of features that best differentiated the stress group from the control group was determined based on the recursive feature elimination (RFE) with cross-validation using the linear SVM. To select the features corresponding to

the optimum number, the shuffled stratified 4-fold cross-validation on the RFE was performed based on the linear SVM. It provided the information on the ranking of features, and the features were selected as the optimal number in the order of highest ranking. Through 100 iterations of this process, the feature importance was determined by calculating the number of times features were selected, and then the features as the optimum number were chosen in the order of high importance.

2.6. Statistical Analysis. All statistical analyses were performed with IBM SPSS Statistics 24 (IBM Corp., Armonk, NY, USA) except for the SVM using scikit learn module [51] in Python software, version 3.6.10 (Python Software Foundation, Wilmington, DE, USA). The concentration of brain metabolites are represented as mean \pm standard deviation. Two-way repeated-measures ANOVA, one of the statistical methods for analyzing time-series data, was performed by comparing the time-dependent change in the concentrations of metabolites between control and stress groups to identify the metabolites that best reflect the acute stress effect. When there were metabolites with statistically significant ($P < 0.05$) differences in the metabolic dynamics between both groups or significant ($P < 0.05$) interactions between time and group, Student's *t*-test for each time point about the metabolites was performed to determine the time point that accurately reflects the acute stress response. False discovery rate (FDR) correction was performed to avoid the multiple comparisons problem of both groups over time.

3. Results

To investigate the temporal effects of acute stress in the mouse hippocampus from a metabolic perspective, all mice in the stress group were under restraint stress for two hours. To objectively evaluate the influence of acute stress, all conditions except for the stress remained the same in both groups. As shown in Figure 2, the metabolites were quantified from ^1H -MRS data of both groups acquired in four consecutive time points (0.8 h: the first time point, 1.6 h: the second time point, 2.4 h: the third time point, 3.2 h: the fourth time point). Among the fifteen metabolites quantified

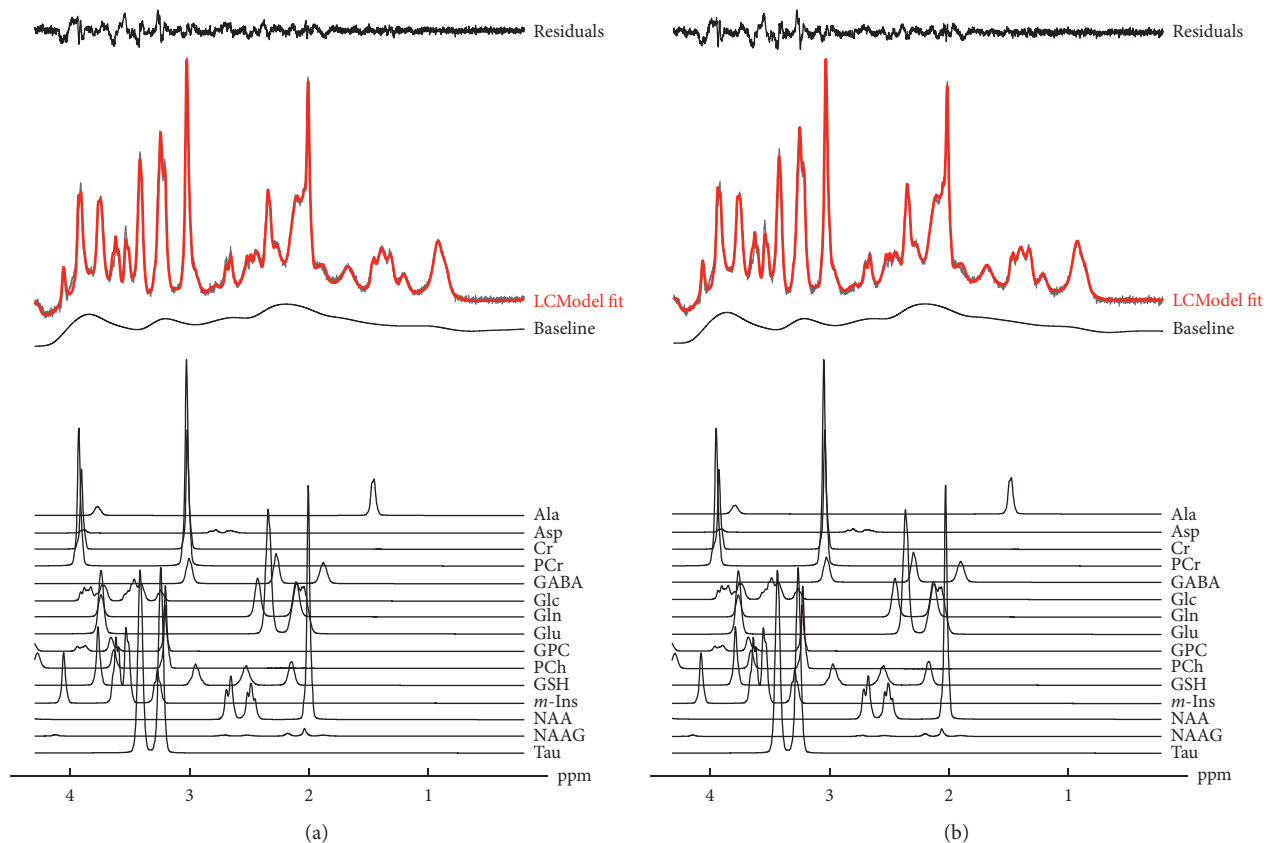


FIGURE 2: Averaged ^1H -MRS raw data (transparent black) and LCMoel fit (red) measured from the mouse hippocampus at 9.4 T Bruker MRI: (a) control and (b) stress. The residuals (top) were the difference between the raw data and the LCMoel fit. The baseline (middle) and each metabolite (bottom) constituting the raw data were represented in the range from 0.2 ppm to 4.3 ppm.

except for Lac (CRLB: 999%), four metabolites were excluded from the statistical analysis based on the comparison of metabolite concentrations in both groups by using all mouse and time points because they did not meet the averaged CRLB criteria: Asp (166%), Glc (144%), GPC (88%), and NAAG (279%).

As shown in Table 1, a total of eleven metabolites were used for the statistical analysis between both groups. Before the analysis, Mauchly's test of sphericity was performed for the time points (within-subject effect), and if the sphericity was violated, the Greenhouse–Geisser and Huynh–Feldt correction were executed using Epsilon. A two-way repeated-measures ANOVA demonstrated a significant difference ($P < 0.05$) in the concentrations of Glu and Ala. The concentrations of Glu and Ala in the stress group were higher than those in the control group at all time points. The effect of time, which is a repetition factor, was statistically significant in most metabolites except for the following metabolites: PCh, Tau, tCr, and tNAA. The interactions between time and group significantly ($P < 0.05$) existed only in Ala, but other metabolites did not.

To make multiple comparisons based on each time point between both groups for Ala and Glu, Student's t -test and FDR correction [52, 53] were performed for each time point including NAA and Gln associated with stress: reduced apical dendrites (NAA) [5, 20] and glutamate-glutamine

(Glu-Gln) cycle (Gln) [54]. Figure 3 illustrates the change in concentration over time for each of the four metabolites. First, Ala was represented in order of time as shown in Figure 3(a): 0.8 h (adjusted $P = 0.02$), 1.6 h (adjusted $P = 0.01$), 2.4 h (adjusted $P = 0.02$), and 3.2 h (adjusted $P = 0.67$); second, Glu in Figure 3(b): 0.8 h (adjusted $P = 0.03$), 1.6 h (adjusted $P = 0.05$), 2.4 h (adjusted $P = 0.08$), and 3.2 h (adjusted $P = 0.08$); third, NAA in Figure 3(c): 0.8 h (adjusted $P = 0.98$), 1.6 h (adjusted $P = 0.74$), 2.4 h (adjusted $P = 0.74$), and 3.2 h (adjusted $P = 0.74$); and finally, Gln in Figure 3(d): 0.8 h (adjusted $P = 0.76$), 1.6 h (adjusted $P = 0.76$), 2.4 h (adjusted $P = 0.76$), and 3.2 h (adjusted $P = 0.76$).

Figure 4 elucidates the optimal number of features, feature importance, and decision boundary in two- and three-dimensional space. Based on the RFE and the cross-validation score that was considered the ratio of correct classification from the linear SVM using repeated stratified 4-fold cross-validation ($n = 100$), the optimal number of features that best explain the effects of acute stress while classifying both groups was three as in Figure 4(a). To select three features among the eleven features, a stratified 4-fold cross-validation that randomly shuffled the data into 3 training sets and 1 test set was used to train the linear SVM and three features with the RFE were determined from the trained linear SVM. Through 100 iterations of this process,

TABLE 1: The effects of acute restraint stress through two-way repeated-measures ANOVA at four time points. Each metabolite was analyzed whether there were effects over time and interaction between time and groups with within-subject effects and whether there was a significant difference between groups due to acute stress.

Metabolites	Within-subject effects		Between-subject effects Group
	Time	Time × group	
Ala	$F_{3,66} = 20.78, P < 0.001^{***}$	$F_{3,66} = 3.38, P = 0.02^*$	$F_{1,22} = 8.95, P = 0.01^*$
Cr	$F_{3,66} = 10.07, P < 0.001^{***}$	$F_{3,66} = 2.00, P = 0.12$	$F_{1,22} = 1.52, P = 0.23$
GABA	$F_{3,66} = 7.81, P < 0.001^{***}$	$F_{3,66} = 1.83, P = 0.15$	$F_{1,22} = 0.69, P = 0.42$
Gln	$F_{3,66} = 16.30, P < 0.001^{***}$	$F_{3,66} = 2.02, P = 0.12$	$F_{1,22} = 0.50, P = 0.49$
Glu	$F_{3,66} = 43.15, P < 0.001^{***}$	$F_{3,66} = 0.09, P = 0.97$	$F_{1,22} = 5.05, P = 0.04^*$
GSH	$F_{2,42,53,16} = 9.53, P < 0.001^{***}$	$F_{2,42,53,16} = 2.05, P = 0.13$	$F_{1,22} = 0.19, P = 0.67$
<i>m</i> -Ins	$F_{3,66} = 7.26, P < 0.001^{***}$	$F_{3,66} = 0.46, P = 0.71$	$F_{1,22} = 2.83, P = 0.11$
NAA	$F_{3,66} = 3.22, P < 0.03^*$	$F_{3,66} = 0.49, P = 0.69$	$F_{1,22} = 0.31, P = 0.58$
PCh	$F_{3,66} = 0.41, P < 0.75$	$F_{3,66} = 0.78, P = 0.51$	$F_{1,22} = 0.88, P = 0.36$
PCr	$F_{3,66} = 6.15, P < 0.001^{***}$	$F_{3,66} = 0.77, P = 0.52$	$F_{1,22} = 0.98, P = 0.33$
Tau	$F_{2,68,59,04} = 0.47, P < 0.68$	$F_{2,68,59,04} = 1.04, P = 0.38$	$F_{1,22} = 2.76, P = 0.11$
Glx	$F_{3,66} = 9.87, P < 0.001^{***}$	$F_{3,66} = 0.60, P = 0.62$	$F_{1,22} = 0.96, P = 0.34$
tCho	$F_{2,60,57,12} = 87.46, P < 0.001^{***}$	$F_{2,60,57,12} = 1.53, P = 0.22$	$F_{1,22} = 0.44, P = 0.51$
tCr	$F_{2,60,56,51} = 0.002, P = 1.00$	$F_{2,60,56,51} = 0.58, P = 0.61$	$F_{1,22} = 3.01, P = 0.10$
tNAA	$F_{3,66} = 2.00, P = 0.12$	$F_{3,66} = 0.33, P = 0.80$	$F_{1,22} = 0.34, P = 0.57$

Glx, glutamate + glutamine; tCho, total choline; tCr, total creatine; tNAA, N-acetylaspargate + N-acetylasparylglutamate.

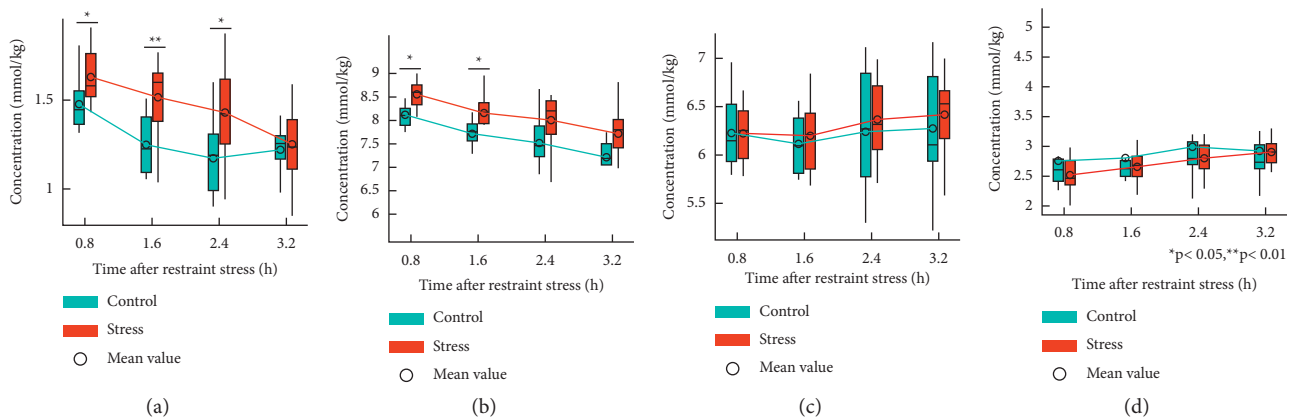


FIGURE 3: Student’s *t*-test at each time point for four metabolites related to acute restraint stress. (a) Ala, (b) Glu, (c) NAA, and (d) Gln. Each of the metabolites was represented by the change of concentration with time after acute stress. The *P* value that was less than or equal to the significance level was considered statistically significant.

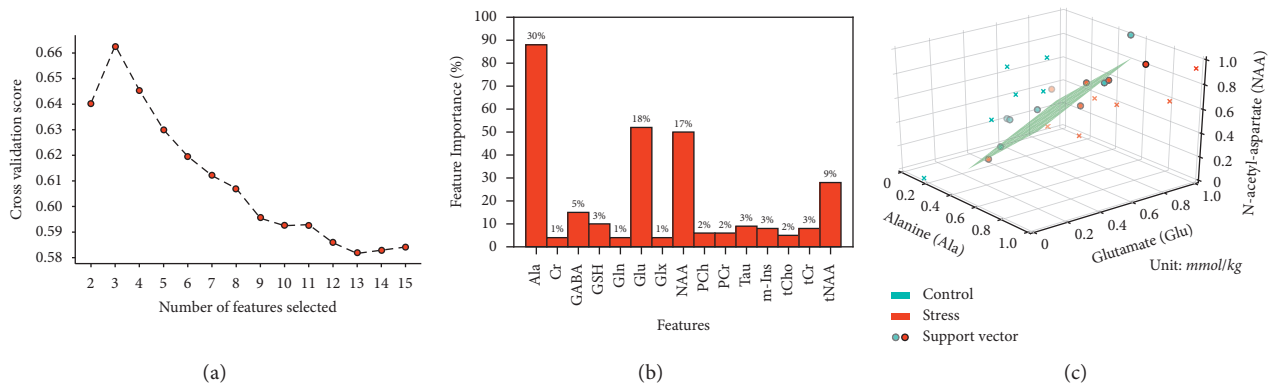


FIGURE 4: Feature importance and decision boundary using the SVM. (a) Optimal number of features that best classified both groups. (b) Feature importance to select the features that best discriminated between both groups. The importance of the feature represented how important the metabolites (i.e., features) were under the influence of acute restraint stress as a quantified quantity. (c) Three-dimensional decision boundary with Ala, Glu, and NAA.

the feature importance ($n_{\text{total}} = 300$), which quantified the influence of each feature to indicate its importance in best distinguishing between both groups, was calculated and three features were selected in order of high ranking based on feature importance as follows: Ala = 30% ($n_{\text{selected}} = 89$), Glu = 18% ($n_{\text{selected}} = 54$), and NAA = 17% ($n_{\text{selected}} = 51$). The feature importance as in Figure 4(b) was indicated by the number of times, and the percentage above the rectangular bar for each feature was the ratio of the number of times to the total times. Figure 4(c) shows the decision boundary that best classified both groups. This was a three-dimensional analysis using Ala, Glu, and NAA identified by the linear SVM.

4. Discussion

The present study revealed that acute restraint stress significantly had a time-based effect on the levels of metabolites in the hippocampus of a mouse. There have been few studies on acute stress over the past decades [10–12, 55, 56] because chronic stress linked to neurological or physiological changes due to an abnormal regulation resulting from a multitude of adaptations to the stress response of the brain has been the focus of interest in stress studies [57, 58]. However, there have been differences in responses to chronic and acute stress [59], and hence, the necessity of studies on acute stress has recently emerged [5].

To our knowledge, the current study using $^1\text{H-MRS}$ was the first attempt to analyze the effect over time on acute restraint stress with the SVM technique providing the following information: (1) acute restraint stress was associated with neurotransmitter transmission through tripartite synapses [54] based on the changes in the concentrations of metabolites including Ala and Glu along with four consecutive time points; (2) the time points that best represented the effect of acute restraint stress were identified; and (3) the three metabolites (Ala, Glu, NAA) were used as an acute stress-specific biomarker, most affected by and vulnerable to acute restraint stress.

Based on the significant difference between both groups using the two-way repeated-measures ANOVA, Ala and Glu are selected for metabolites associated with acute restraint stress. Acute restraint stress is a single extreme stressor, and the acute stress response resulting from the stressor is an immediate neurochemical reaction to adapt for survival [7]. Acute restraint stress activates the hypothalamic-pituitary-adrenal axis. The hypothalamus releases the corticotropin-releasing hormone (CRH). CRH stimulates the pituitary secretion of adrenocorticotrophic hormone (ACTH), which activates the release of glucocorticoids such as corticosterone (CORT) from the adrenal glands [60–62]. CORT enters the hippocampus via the bloodstream and combines with the glucocorticoid receptors to release an excitatory neurotransmitter, Glu, from the presynaptic membrane of the neuron [63]. Although Glu has been implicated in stress, the role of Ala in the stress response is unclear. The physiological characteristics of Ala associated with stress suggest that it may act as a regulator of the acute stress response [64]. First, L-alanine is mediated via the glycine receptor and glycine is

considered an inhibitory neurotransmitter that inhibits the sensitivity of the neurons in the brain region with the highest CRH concentration. Second, L-alanine produces β -alanine, considered to have an antistress effect, as a by-product of the reaction to convert to pyruvate. β -alanine increases the amount of carnosine that enhances the resilience to stress and regulates the stress response in the mouse hypothalamus [55, 65]. Finally, using alanine transaminase and ammonium ions from α -ketoglutarate, L-alanine provides pyruvate and Glu through the Glu-Gln cycling during pyruvate conversion, and pyruvate is converted into glucose [66, 67]. The metabolism involved in converting L-alanine to glucose through pyruvate may be responsible for the sedative effects of L-alanine [64, 68]. Based on the above evidence, acute stress can increase the concentrations of Ala and Glu. This finding is consistent with the results of the present study, which show higher concentrations of Ala and Glu in the stress group than in the control group.

In the control group, the concentration of Glu decreases over time, the one of Ala shows a trend of decreasing and then recovering, and the one of Gln shows a constant trend. The brain is trying to reduce the Glu in the extracellular space (ECS) such as synaptic clefts as much as possible to the normal state [13, 69]. Conversely, the concentrations of Ala and Glu decrease over time in the stress group and the one of Gln increases over time. As a result of acute stress, more glutamate is produced and a pattern that decreases with time is like the one of the control group due to trying to reduce it as much as possible. Glu-Gln cycling in the hippocampus of the mouse brain can be described as the transport of Glu acting as the excitatory neurotransmitter and Gln forming through the amidation of glutamate in the tripartite synapses [54, 70–72]. Thus, Gln production and Glu decomposition occur in astrocytes, and the opposite effects occur in neurons via Glu-Gln cycling [67]. The tripartite synapses consist of presynaptic and postsynaptic neurons and astrocytes. Stress stimulates the presynaptic neuron to release Glu into the ECS. Subsequently, Glu is transported via glutamate transporter-1 (GLT-1) to neighboring astrocytes as a glial cell type adjacent to the neuron, where it is amidated to Gln using ammonium ions and converted into a nontoxic neutral amino acid. Elimination of Glu controls its ECS concentration, enables the maintenance of homeostasis in the tripartite synapses, and prevents excitotoxicity resulting from Glu accumulation in the ECS [54, 73]. Impaired astrocyte and GLT-1 function can produce symptoms of neurodegenerative diseases and mental disorders such as depression [54, 74–76]. Thus, the opposite effects of Glu and Gln over time can be attributed to the Glu-Gln cycle that is responsible for Glu removal and Glu synthesis in the ECS following acute stress. As the Ala cycle is associated with the Glu-Gln cycle [77], Ala may represent the same results as Glu. The continuous decrease in the concentration of Ala and Glu over time following acute stress can be explained as follows: (1) the estimate of astrocyte-to-neuron ratio in the hippocampus is 0.68 [78], and therefore, several hippocampal astrocytes decompose Ala into pyruvate and convert Glu to Gln compared to synthesis of Gln via Glu in neurons [67]; (2) the physiological responses during acute stress

increase the energy demands for various neural activities, such as glutamatergic neurotransmission, including Glu-Gln cycling. The energy required for Glu cycling in Glu-Gln cycling between astrocytes and neurons can be estimated as three ATP molecules per glutamate molecule, approximately [63, 79, 80]. Thus, lactate dehydrogenase converts the pyruvate caused by Ala to Lac, which is used as a material for energy metabolism in astrocytes [63, 67, 81].

Although there is no statistically significant difference, Gln and NAA related to acute stress are added. Gln is directly related through the Glu-Gln cycle and NAA is associated with the effects of acute stress such as reduced neurons based on recent studies [5, 20, 27]. Comparing the concentrations of the above four metabolites between both groups at each time point, Ala differs in the first, second, and third time points, and Glu differs in the first time point after FDR correction, while NAA and Gln do not differ at every point in time. After acute stress is induced, Ala is found to have a time-dependent effect on acute stress for up to an hour and a half and Glu for half an hour. This observation demonstrates that the acute stress response and its effect varies over time, which can overcome the limitation of the existing end-point analysis methods due to several adaptive changes occurring during acute stress responses in many animal studies [10, 11, 13], and provides a deep understanding of the stress response for important time points and related metabolism with time after acute stress. Moreover, recent studies have shown that the effects of acute stress over time can be divided as short-term and long-term effects, necessitating a consideration of the stress response itself [5, 58, 82]. The time-lasting effects can cause morphological changes such as remodeling and atrophy of apical dendrites in the hippocampus [4, 18, 83–86]. An impaired physiological and functional response to stress may lead to the development of stress-related disorders in the brain [20]. These time-related short-term and long-term effects provide an understanding of acute stress response mechanisms in the brain from the metabolic viewpoint [5, 28, 87]. This observation may help us to identify turning points (recovery via adaptation) [5, 58] and sensitivity (vulnerable vs. resilient) [88, 89] for stress response by evaluating the time-based effects of acute stress and monitoring maladaptive acute stress responses that may induce stress-related brain disorders.

Because of the small sample size, the AUC is used for the selection of features basing on the linear SVM to reduce the bias such as the difference between animals rather than using absolute concentrations at four time points. The AUC of each metabolite is calculated through the integration based on the trapezoidal method under the concentration curve of four time points, and it reflects the change over time and is similar to the averaged concentration of all time points. Using the cross-validation and RFE of the linear SVM based on the AUC in each feature as a metabolite, the three features (Ala, Glu, and NAA) are selected in the order of high importance in Figure 4(b). This indicates that the three metabolites as stress-specific metabolites are important for acute stress response and best represent the temporal effects of acute stress. Using the RFE and cross-validation with the

linear SVM rather than the two-way repeated-measures ANOVA and Student's *t*-test adds one additional metabolite (NAA) that differentiates the effects of acute stress. Based on the recent studies [5, 27], NAA is demonstrated to be a metabolite affecting the effects of acute stress as well as the third most important one as shown in Figure 4(b), although there is no statistically significant difference. The decision boundary that best classifies between both groups using three metabolites, one metabolite is one dimension, is shown in Figure 4(c). This can be obtained from a different perspective than the information obtained by comparing and analyzing the concentration itself and can be used as a biological indicator or stress-specific biomarker to characterize the effect of acute stress in the future.

There are a few limitations to the present study. First, the simulated lipid and macromolecule is used because it cannot be acquired under the same conditions as before due to breakdowns, repairs, and upgrades of the MRI machine. This indicates that the concentration of metabolites can be under- and overquantified rather than precisely quantified. Second, the sample size is too small, which may have resulted in bias due to various reasons, including differences between animals. Third, the time resolution is low. The current study takes 30 minutes to acquire a single point of time. As there is a 30-minute interval for each time point, we cannot evaluate the physiological responses occurring within the interval from a metabolic point of view. Fourth, the experimental animals are anesthetized for a prolonged period to acquire ¹H-MRS data. Prolonged administration of isoflurane to obtain all time points can influence several metabolites. Finally, the total acquisition time may have been short for analyzing the long-term effects of acute stress, which can only be assessed in part in the overall response. Despite these limitations, the current study can provide useful information such as stress-specific or stress-related metabolites and important time points after acute stress on the temporal effects of acute stress.

5. Conclusions

This study analyzes the effect of acute restraint stress on the metabolite levels in the mouse hippocampus over time. We found the following results: (1) there was a significant difference in Ala and Glu levels due to acute restraint stress; (2) among the four time points, the statistical difference between both groups occurred in the preceding three time points in Ala and the first time point in Glu after acute restraint stress; and (3) Ala, Glu, and NAA, which best classified the two groups, were selected with SVM as an optimal combination of metabolites. Our findings indicate the effects of acute stress over time, providing information on the timing of analysis after acute stress. Furthermore, the stress-specific biomarker, a combination of three metabolites (Ala, Glu, and NAA), best explains the influence of acute stress. Moreover, this study may provide a better understanding of the acute stress response mechanisms and present new insights into whether laboratory animals such as rodents are vulnerable or resilient to acute stress from a metabolic point of view.

Data Availability

The analyzed data for the metabolites used to support the findings of this study are available from the corresponding author upon reasonable request.

Conflicts of Interest

The authors declare no conflicts of interest.

Acknowledgments

This research was supported by the Brain Research Program of the National Research Foundation (NRF) funded by the Korean Government (MSIT) (2016M3C7A1905385).

Supplementary Materials

Figure S1: averaged proton MRS raw data, LCModel fit, and quantified metabolites at the first time point. Figure S2: averaged proton MRS raw data, LCModel fit, and quantified metabolites at the second time point. Figure S3: averaged proton MRS raw data, LCModel fit, and quantified metabolites at the third time point. Figure S4: averaged proton MRS raw data, LCModel fit, and quantified metabolites at the fourth time point. Table S1: statistical comparison (Wilcoxon rank sum test with FDR correction) by group of baselines per ppm ($P < 0.05$). (*Supplementary Materials*)

References

- [1] H. Selye, "A personal message from hans selye," *Journal of Extension*, vol. 18, no. 3, pp. 6–11, 1980.
- [2] I. N. Karatsoreos and B. S. McEwen, "Stress and allostasis," in *Handbook of Behavioral Medicine*, A. Steptoe, Ed., Springer, Berlin, Germany, pp. 649–658, 2010.
- [3] M. Popoli, Z. Yan, B. S. McEwen, and G. Sanacora, "The stressed synapse: the impact of stress and glucocorticoids on glutamate transmission," *Nature Reviews Neuroscience*, vol. 13, no. 1, pp. 22–37, 2012.
- [4] B. S. McEwen, N. P. Bowles, J. D. Gray et al., "Mechanisms of stress in the brain," *Nature Neuroscience*, vol. 18, no. 10, pp. 1353–1363, 2015.
- [5] L. Musazzi, P. Tornese, N. Sala, and M. Popoli, "Acute or chronic? a stressful question," *Trends in Neurosciences*, vol. 40, no. 9, pp. 525–535, 2017.
- [6] V. K. Patchev and A. V. Patchev, "Experimental models of stress," *Dialogues in Clinical Neuroscience*, vol. 8, no. 4, pp. 417–432, 2006.
- [7] T. B. Franklin, B. J. Saab, and I. M. Mansuy, "Neural mechanisms of stress resilience and vulnerability," *Neuron*, vol. 75, no. 5, pp. 747–761, 2012.
- [8] K. J. McLaughlin, J. L. Gomez, S. E. Baran, and C. D. Conrad, "The effects of chronic stress on hippocampal morphology and function: an evaluation of chronic restraint paradigms," *Brain Research*, vol. 1161, pp. 56–64, 2007.
- [9] D. Knox, S. A. Perrine, S. A. George, M. P. Galloway, and I. Liberzon, "Single prolonged stress decreases glutamate, glutamine, and creatine concentrations in the rat medial prefrontal cortex," *Neuroscience Letters*, vol. 480, no. 1, pp. 16–20, 2010.
- [10] G. Hasler, J. W. van der Veen, C. Grillon, W. C. Drevets, and J. Shen, "Effect of acute psychological stress on prefrontal GABA concentration determined by proton magnetic resonance spectroscopy," *American Journal of Psychiatry*, vol. 167, no. 10, pp. 1226–1231, 2010.
- [11] S.-Y. Kim, E.-J. Jang, K. S. Hong et al., "Acute restraint-mediated increases in glutamate levels in the rat brain: an in vivo 1H-MRS study at 4.7 T," *Neurochemical Research*, vol. 37, no. 4, pp. 740–748, 2012.
- [12] A. L. Colín-González, H. Becerril, B. R. Flores-Reyes et al., "Acute restraint stress reduces hippocampal oxidative damage and behavior in rats: effect of S-allyl cysteine," *Life Sciences*, vol. 135, pp. 165–172, 2015.
- [13] L. C. Houtepen, R. R. Schür, J. P. Wijnen et al., "Acute stress effects on GABA and glutamate levels in the prefrontal cortex: a 7T 1 H magnetic resonance spectroscopy study," *NeuroImage: Clinical*, vol. 14, pp. 195–200, 2017.
- [14] B. S. McEwen, "Protective and damaging effects of stress mediators," *New England Journal of Medicine*, vol. 338, no. 3, pp. 171–179, 1998.
- [15] B. S. McEwen, "Stress and hippocampal plasticity," *Annual Review of Neuroscience*, vol. 22, no. 1, pp. 105–122, 1999.
- [16] C. D. Conrad, R. L. Wright, and K. J. McLaughlin, "Stress and vulnerability to brain damage," in *Encyclopedia of Neuroscience*, L. R. Squire, Ed., Elsevier, Amsterdam, Netherlands, pp. 481–488, 2009.
- [17] Y. Chen, C. S. Rex, C. J. Rice et al., "Correlated memory defects and hippocampal dendritic spine loss after acute stress involve corticotropin-releasing hormone signaling," *Proceedings of the National Academy of Sciences*, vol. 107, no. 29, pp. 13123–13128, 2010.
- [18] G. Sanacora, G. Treccani, and M. Popoli, "Towards a glutamate hypothesis of depression: an emerging frontier of neuropsychopharmacology for mood disorders," *Neuropharmacology*, vol. 62, no. 1, pp. 63–77, 2012.
- [19] C. Rocher, M. Spedding, C. Munoz, and T. M. Jay, "Acute stress-induced changes in hippocampal/prefrontal circuits in rats: effects of antidepressants," *Cerebral Cortex*, vol. 14, no. 2, pp. 224–229, 2004.
- [20] L. Musazzi, P. Tornese, N. Sala, and M. Popoli, "What acute stress protocols can tell us about PTSD and stress-related neuropsychiatric disorders," *Frontiers in Pharmacology*, vol. 9, Article ID 758, 2018.
- [21] M. T. Lowy, L. Wittenberg, and B. K. Yamamoto, "Effect of acute stress on hippocampal glutamate levels and spectrin proteolysis in young and aged rats," *Journal of Neurochemistry*, vol. 65, no. 1, pp. 268–274, 1995.
- [22] R. M. Sapolsky, "The possibility of neurotoxicity in the hippocampus in major depression: a primer on neuron death," *Biological Psychiatry*, vol. 48, no. 8, pp. 755–765, 2000.
- [23] A. Kumar, R. L. Singh, and G. N. Babu, "Cell death mechanisms in the early stages of acute glutamate neurotoxicity," *Neuroscience Research*, vol. 66, no. 3, pp. 271–278, 2010.
- [24] J. Lewerenz and P. Maher, "Chronic glutamate toxicity in neurodegenerative diseases—what is the evidence?" *Frontiers in Neuroscience*, vol. 9, Article ID 469, 2015.
- [25] B. Czéh, T. Michaelis, T. Watanabe et al., "Stress-induced changes in cerebral metabolites, hippocampal volume, and cell proliferation are prevented by antidepressant treatment with tianeptine," *Proceedings of the National Academy of Sciences*, vol. 98, no. 22, pp. 12796–12801, 2001.
- [26] E. R. de Kloet, M. Joëls, and F. Holsboer, "Stress and the brain: from adaptation to disease," *Nature Reviews Neuroscience*, vol. 6, no. 6, pp. 463–475, 2005.

- [27] W. Zhang, M. M. Hashemi, R. Kaldewaij et al., "Acute stress alters the 'default' brain processing," *NeuroImage*, vol. 189, pp. 870–877, 2019.
- [28] F. S. Dhabhar, "The short-term stress response - mother nature's mechanism for enhancing protection and performance under conditions of threat, challenge, and opportunity," *Frontiers in Neuroendocrinology*, vol. 49, pp. 175–192, 2018.
- [29] S. Gandhi, M. M. Devi, S. Pal, R. P. Tripathi, and S. Khushu, "Metabolic regulatory variations in rats due to acute cold stress & *tinospora cordifolia* intervention: high resolution ^1H NMR approach," *Metabolomics*, vol. 8, no. 3, pp. 444–453, 2012.
- [30] B. Shi, J. Tian, H. Xiang et al., "A ^1H -NMR plasma metabolomic study of acute and chronic stress models of depression in rats," *Behavioural Brain Research*, vol. 241, pp. 86–91, 2013.
- [31] K. Gapp, A. Corcoba, G. van Steenwyk, I. M. Mansuy, and J. M. Duarte, "Brain metabolic alterations in mice subjected to postnatal traumatic stress and in their offspring," *Journal of Cerebral Blood Flow and Metabolism*, vol. 37, no. 7, pp. 2423–2432, 2017.
- [32] M.-S. Lee, Y.-H. Kim, W.-S. Park et al., "Temporal variability of glucocorticoid receptor activity is functionally important for the therapeutic action of fluoxetine in the hippocampus," *Molecular Psychiatry*, vol. 21, no. 2, pp. 252–260, 2016.
- [33] S. Aruna and S. P. Rajagopalan, "A novel SVM based CSSFFS feature selection algorithm for detecting breast cancer," *International journal of computer applications*, vol. 31, no. 8, 2011.
- [34] S. Huang, N. Cai, P. P. Pacheco, S. Narrandes, Y. Wang, and W. Xu, "Applications of support vector machine (SVM) learning in cancer genomics," *Cancer Genomics and Proteomics*, vol. 15, no. 1, pp. 41–51, 2018.
- [35] R. H. Bonneau, J. F. Sheridan, N. Feng, and R. Glaser, "Stress-induced modulation of the primary cellular immune response to herpes simplex virus infection is mediated by both adrenal-dependent and independent mechanisms," *Journal of Neuroimmunology*, vol. 42, no. 2, pp. 167–176, 1993.
- [36] K. Iwakabe, M. Shimada, A. Ohta et al., "The restraint stress drives a shift in Th1/Th2 balance toward Th2-dominant immunity in mice," *Immunology Letters*, vol. 62, no. 1, pp. 39–43, 1998.
- [37] A. C. Caro, F. C. Hankenson, and J. O. Marx, "Comparison of thermoregulatory devices used during anesthesia of C57BL/6 mice and correlations between body temperature and physiologic parameters," *Journal of the American Association for Laboratory Animal Science*, vol. 52, no. 5, pp. 577–583, 2013.
- [38] M. Talan, "Body temperature of C57BL/6j mice with age," *Experimental Gerontology*, vol. 19, no. 1, pp. 25–29, 1984.
- [39] I. Tkáč, Z. Starčuk, I. Y. Choi, and R. Gruetter, "In vivo ^1H NMR spectroscopy of rat brain at 1 ms echo time," *Magnetic Resonance in Medicine*, vol. 41, no. 4, pp. 649–656, 1999.
- [40] J. F. A. Jansen, W. H. Backes, K. Nicolay, and M. E. Kooi, " ^1H MR spectroscopy of the brain: absolute quantification of metabolites," *Radiology*, vol. 240, no. 2, pp. 318–332, 2006.
- [41] Y. Zhang, S. Marengo, and J. Shen, "Correction of frequency and phase variations induced by eddy currents in localized spectroscopy with multiple echo times," *Magnetic Resonance in Medicine*, vol. 58, no. 1, pp. 174–178, 2007.
- [42] K.-N. Kim, Y.-B. Kim, and Z.-H. Cho, "Improvement of a 4-channel spiral-loop RF coil array for TMJ MR imaging at 7T," *Journal of the Korean Society of Magnetic Resonance in Medicine*, vol. 16, no. 2, pp. 103–114, 2012.
- [43] S. W. Provencher, "Estimation of metabolite concentrations from localized in vivo proton NMR spectra," *Magnetic Resonance in Medicine*, vol. 30, no. 6, pp. 672–679, 1993.
- [44] S. W. Provencher, "Automatic quantitation of localized in vivo ^1H spectra with LCMoDel," *NMR in Biomedicine*, vol. 14, no. 4, pp. 260–264, 2001.
- [45] J. K. Choi, I. Carreras, A. Dedeoglu, and B. G. Jenkins, "Detection of increased scyllo-inositol in brain with magnetic resonance spectroscopy after dietary supplementation in Alzheimer's disease mouse models," *Neuropharmacology*, vol. 59, no. 4-5, pp. 353–357, 2010.
- [46] V. Mlynárik, C. Cudalbu, L. Xin, and R. Gruetter, " ^1H NMR spectroscopy of rat brain in vivo at 14.1 Tesla: improvements in quantification of the neurochemical profile," *Journal of Magnetic Resonance*, vol. 194, no. 2, pp. 163–168, 2008.
- [47] V. Govindaraju, K. Young, and A. A. Maudsley, "Proton NMR chemical shifts and coupling constants for brain metabolites," *NMR in Biomedicine*, vol. 13, no. 3, pp. 129–153, 2000.
- [48] M. Terpstra and R. Gruetter, " ^1H NMR detection of vitamin C in human brain in vivo," *Magnetic Resonance in Medicine*, vol. 51, no. 2, pp. 225–229, 2004.
- [49] S. W. Provencher, *LCModel & LCMgui User's Manual*, 2021, <http://s-provencher.com/pub/LCModel/manual/manual.pdf>.
- [50] C. Qi, Y. Li, X. Fan et al., "A quantitative SVM approach potentially improves the accuracy of magnetic resonance spectroscopy in the preoperative evaluation of the grades of diffuse gliomas," *NeuroImage: Clinical*, vol. 23, Article ID 101835, 2019.
- [51] F. Pedregosa, G. Varoquaux, A. Gramfort et al., "Scikit-learn: machine learning in python," *Journal of Machine Learning Research*, vol. 12, pp. 2825–2830, 2011.
- [52] Y. Benjamini and Y. Hochberg, "Controlling the false discovery rate: a practical and powerful approach to multiple testing," *Journal of the Royal Statistical Society: Series B*, vol. 57, no. 1, pp. 289–300, 1995.
- [53] D. Yekutieli and Y. Benjamini, "Resampling-based false discovery rate controlling multiple test procedures for correlated test statistics," *Journal of Statistical Planning and Inference*, vol. 82, no. 1-2, pp. 171–196, 1999.
- [54] V. Rappeneau, A. Blaker, J. R. Petro, B. K. Yamamoto, and A. Shimamoto, "Disruption of the glutamate–glutamine cycle involving astrocytes in an animal model of depression for males and females," *Frontiers in Behavioral Neuroscience*, vol. 10, Article ID 231, 2016.
- [55] J. R. Hoffman, A. Varanoske, and J. R. Stout, "Effects of β -alanine supplementation on carnosine elevation and physiological performance," *Advances in Food and Nutrition Research*, vol. 84, pp. 183–206, 2018.
- [56] M. Wang, V. S. Ramasamy, M. Samidurai, and J. Jo, "Acute restraint stress reverses impaired LTP in the hippocampal CA1 region in mouse models of Alzheimer's disease," *Scientific Reports*, vol. 9, no. 1, pp. 10955–10959, 2019.
- [57] B. S. McEwen and P. J. Gianaros, "Central role of the brain in stress and adaptation: links to socioeconomic status, health, and disease," *Annals of the New York Academy of Sciences*, vol. 1186, no. 1, pp. 190–222, 2010.
- [58] L. Musazzi, P. Tornese, N. Sala, and M. Popoli, "Acute stress is not acute: sustained enhancement of glutamate release after acute stress involves readily releasable pool size and synapsin I activation," *Molecular Psychiatry*, vol. 22, no. 9, pp. 1226–1227, 2017.
- [59] C. R. Teague, F. S. Dhabhar, R. H. Barton et al., "Metabonomic studies on the physiological effects of acute and chronic

- psychological stress in sprague-dawley rats," *Journal of Proteome Research*, vol. 6, no. 6, pp. 2080–2093, 2007.
- [60] B. M. Kudielka, N. C. Schommer, D. H. Hellhammer, and C. Kirschbaum, "Acute HPA axis responses, heart rate, and mood changes to psychosocial stress (TSST) in humans at different times of day," *Psychoneuroendocrinology*, vol. 29, no. 8, pp. 983–992, 2004.
- [61] B. M. Kudielka and C. Kirschbaum, "Sex differences in HPA axis responses to stress: a review," *Biological Psychology*, vol. 69, no. 1, pp. 113–132, 2005.
- [62] A. L. Russell, J. G. Tasker, A. B. Lucion et al., "Factors promoting vulnerability to dysregulated stress reactivity and stress-related disease," *Journal of Neuroendocrinology*, vol. 30, no. 10, Article ID e12641, 2018.
- [63] D. M. Osborne, J. Pearson-Leary, and E. C. McNay, "The neuroenergetics of stress hormones in the hippocampus and implications for memory," *Frontiers in Neuroscience*, vol. 9, Article ID 164, 2015.
- [64] I. Kurauchi, H. Yamane, Y. Tsuneyoshi, D. M. Denbow, and M. Furuse, "Central L-alanine reduces energy expenditure with a hypnotic effect under an acute stressful condition in neonatal chicks," *Amino Acids*, vol. 36, no. 1, pp. 131–135, 2009.
- [65] B. Tsoi, R.-R. He, D.-H. Yang et al., "Carnosine ameliorates stress-induced glucose metabolism disorder in restrained mice," *Journal of Pharmacological Sciences*, vol. 117, no. 4, pp. 223–229, 2011.
- [66] L. Stryer, M. B. Jeremy, and L. John, "Protein turnover and amino acid catabolism," in *Biochemistry*, pp. 633–662, W. H. Freeman and Company, New York, NY, USA, 2002.
- [67] E. Somersalo and D. Calvetti, "Quantitative in silico analysis of neurotransmitter pathways under steady state conditions," *Frontiers in Endocrinology*, vol. 4, Article ID 137, 2013.
- [68] M. Asechi, I. Kurauchi, S. Tomonaga et al., "Relationships between the sedative and hypnotic effects of intracerebroventricular administration of L-serine and its metabolites, pyruvate and the derivative amino acids contents in the neonatal chicks under acute stressful conditions," *Amino Acids*, vol. 34, no. 1, pp. 55–60, 2008.
- [69] Y. Daikhin and M. Yudkoff, "Compartmentation of brain glutamate metabolism in neurons and glia," *Journal of Nutrition*, vol. 130, no. 4, pp. 1026S–1031S, 2000.
- [70] S. Bröer and N. Brookes, "Transfer of glutamine between astrocytes and neurons," *Journal of Neurochemistry*, vol. 77, no. 3, pp. 705–719, 2001.
- [71] L. K. Bak, A. Schousboe, and H. S. Waagepetersen, "The glutamate/GABA-glutamine cycle: aspects of transport, neurotransmitter homeostasis and ammonia transfer," *Journal of Neurochemistry*, vol. 98, no. 3, pp. 641–653, 2006.
- [72] J. Albrecht, U. Sonnewald, H. S. Waagepetersen, and A. Schousboe, "Glutamine in the central nervous system: function and dysfunction," *Frontiers in Bioscience: A Journal and Virtual Library*, vol. 12, no. 332, pp. 332–343, Article ID e43, 2007.
- [73] J. D. Rothstein, M. Dykes-Hoberg, C. A. Pardo et al., "Knockout of glutamate transporters reveals a major role for astroglial transport in excitotoxicity and clearance of glutamate," *Neuron*, vol. 16, no. 3, pp. 675–686, 1996.
- [74] M. Banasr, G. M. I. Chowdhury, R. Terwilliger et al., "Glial pathology in an animal model of depression: reversal of stress-induced cellular, metabolic and behavioral deficits by the glutamate-modulating drug riluzole," *Molecular Psychiatry*, vol. 15, no. 5, pp. 501–511, 2010.
- [75] M. D. Scofield and P. W. Kalivas, "Astrocytic dysfunction and addiction: consequences of impaired glutamate homeostasis," *The Neuroscientist*, vol. 20, no. 6, pp. 610–622, 2014.
- [76] A. R. Filous and J. Silver, "Targeting astrocytes in CNS injury and disease: a translational research approach," *Progress in Neurobiology*, vol. 144, pp. 173–187, 2016.
- [77] S. Bröer, A. Bröer, J. T. Hansen et al., "Alanine metabolism, transport, and cycling in the brain," *Journal of Neurochemistry*, vol. 102, no. 6, pp. 1758–1770, 2007.
- [78] D. Keller, C. Erö, and H. Markram, "Cell densities in the mouse brain: a systematic review," *Frontiers in Neuroanatomy*, vol. 12, Article ID 83, 2018.
- [79] D. Attwell and S. B. Laughlin, "An energy budget for signaling in the grey matter of the brain," *Journal of Cerebral Blood Flow and Metabolism*, vol. 21, no. 10, pp. 1133–1145, 2001.
- [80] J. J. Harris, R. Jolivet, and D. Attwell, "Synaptic energy use and supply," *Neuron*, vol. 75, no. 5, pp. 762–777, 2012.
- [81] A. J. L. Cooper, "The role of glutamine synthetase and glutamate dehydrogenase in cerebral ammonia homeostasis," *Neurochemical Research*, vol. 37, no. 11, pp. 2439–2455, 2012.
- [82] J. Bagley and B. Moghaddam, "Temporal dynamics of glutamate efflux in the prefrontal cortex and in the hippocampus following repeated stress: effects of pretreatment with saline or diazepam," *Neuroscience*, vol. 77, no. 1, pp. 65–73, 1997.
- [83] J. M. Gorman and J. P. Docherty, "A hypothesized role for dendritic remodeling in the etiology of mood and anxiety disorders," *Journal of Neuropsychiatry and Clinical Neurosciences*, vol. 22, no. 3, pp. 256–264, 2010.
- [84] R. S. Duman and G. K. Aghajanian, "Synaptic dysfunction in depression: potential therapeutic targets," *Science*, vol. 338, no. 6103, pp. 68–72, 2012.
- [85] N. Sousa and O. F. X. Almeida, "Disconnection and reconnection: the morphological basis of (mal)adaptation to stress," *Trends in Neurosciences*, vol. 35, no. 12, pp. 742–751, 2012.
- [86] N. Nava, G. Treccani, A. Alabsi et al., "Temporal dynamics of acute stress-induced dendritic remodeling in medial prefrontal cortex and the protective effect of desipramine," *Cerebral Cortex*, vol. 27, no. 1, pp. 694–705, 2017.
- [87] Y. Li, X. Hou, D. Wei et al., "Long-term effects of acute stress on the prefrontal-limbic system in the healthy adult," *PLoS One*, vol. 12, no. 1, Article ID e0168315, 2017.
- [88] N. P. Daskalakis, R. Yehuda, and D. M. Diamond, "Animal models in translational studies of PTSD," *Psychoneuroendocrinology*, vol. 38, no. 9, pp. 1895–1911, 2013.
- [89] N. P. Daskalakis, R. Yehuda, and D. M. Diamond, "Mind the gap: glucocorticoids modulate hippocampal glutamate tone underlying individual differences in stress susceptibility," *Molecular Psychiatry*, vol. 20, no. 6, pp. 755–763, 2015.